Wojciech PIETROWSKI

Poznan University of Technology, Institute of Electrical Engineering and Electronics

Wavelet analysis of axial flux in an induction machine on no-load test

Abstract. *The application of a wavelet analysis of axial flux in an induction machine has been presented. The axial flux occurs when there is any kind of asymmetry in a machine. In this paper the asymmetry of stator windings has been investigated. A detailed analysis of the voltage induced in a search coil was made using the Discrete Fourier Transform (DFT), the Discrete Stationary Wavelet Transform (DSWT), and the Wavelet Packet Decomposition (WPD). On the basis of the results it can be concluded that the DSWT can be used in the de-noising process and the WPD can be used in the preparation of the input vector for artificial neural network in a faults detector*

Streszczenie. *W artykule zaprezentowano falkową analizę strumienia osiowego silnika indukcyjnego. Strumień osiowy powstaje w przypadku pojawienia się asymetrii w maszynie. Skoncentrowano się na badaniu wpływu asymetrii uzwojenia stojana na strumień osiowy. Do analizy wyników pomiarów zastosowano Dyskretną Transformatę Fouriera (DFT), Dyskretną Stacjonarną Analizę Falkową (DSWT), Pakietową Analizę Falkową (WPD). Na podstawie otrzymanych wyników można stwierdzić przydatność DSWT do usunięcia szumów natomiast WPD do przygotowania wektora wejściowego neuronowego detektora uszkodzeń. (**Falkowa analiza strumienia osiowego silnika indukcyjnego pracującego na biegu jałowym**).*

Keywords: wavelet analysis, faults, induction machine, axial flux.
Słowa kluczowe: analiza falkowa, uszkodzenia, maszyna indukcyjna, strumień osiowy.

Introduction

In the diagnostics of electrical machines we look for diagnostics methods that do not interfere with the operation of the machine. The most popular methods are based on the measurements of the phase currents, the pulsation of the torque, or the vibrations of the machine. The measured signals can be analyzed using the following methods: the Motor Current Signatures Analysis (MCSA), the Extended Park's Vector Approach (EPVA) and the Discrete Wavelet Transform [1, 2]. On the basis of those measurements and the results of their analysis, it can be concluded about faults in the machine, i.e. in the stator and rotor windings, or in the bearings. The majority of diagnostics method can identify the condition of the machine after major faults had occurred. The difficulty in faults identifying is separation of the diagnostics symptoms from the measured signals. For faults identification the dedicated Artificial Neural Network (ANN) can be used [3, 4]. The disadvantage of using the ANN is the necessity to form a proper data set for the training process. The data set should include patterns of all faults in machine.

The faults on the electric circuit of the windings (short-turns, broken bars) as well as on the magnetic circuit rotor eccentricity) cause asymmetry in the machine [5]. One of the asymmetry symptoms is an axial flux [6]. It arises when the sum of phase fluxes is not equal to zero.

Measurement of axial flux

A 3-phase squirrel cage induction machine has been selected for the experiment. The rated values are: supply voltage U_N=380V, power P_N=2.2 kW, speed n_N=1420 rpm.

The measurements of the axial flux were made with a dedicated search coil. The coil was mounted at the end-turn area of the stator winding. The presents of the search coil can be neglected because of the very high self-resistance of the measuring device connected to the coil. The advantage of using a search coil is low cost, but on the other hand the mounting process requires the end shield of the machine to be removed. In Fig.1. the pictorial view of a search coil is presented.

In order to model the asymmetry in the machine, the winding of each phase was divided into electrically separated parts. The ends of each part were taken out of the machine. The scheme of the stator winding parts is presented in Fig.2. The share of each part in stator winding is presented in Table 1. The measurements of voltage U_C were taken for the cases of stator winding asymmetry presented in Table 2. Because of a significant reduction in the number of stator winding turns the supply voltage was reduced to U=150V. The machine worked at no-loaded test, i.e. without external load torque. The rotational speed during the measurements was practically constant and averaged out 1495 rpm. The recorded waveforms of the coil voltage U_C for each case presented in Table 2 (from P1 to P6) are shown in Fig. 3.

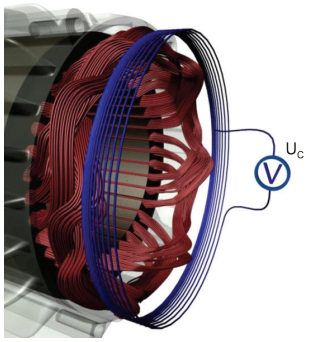

Fig. 1. The pictorial view of search coil

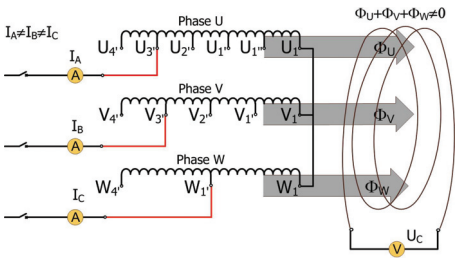

Fig. 2. The scheme of stator winding parts

Table 1. The share of parts in stator winding

Part	Phase U	Phase V	Phase W
1 – 4'	100 %	100%	100%
1 – 3'	80%	75%	n.a.
1 – 2'	60%	50%	n.a.
1 – 1'	40%	25%	50%
1 – 1''	20%	n.a.	n.a.

Table 2. Cases of stator winding asymmetry

Case	Phase U	Phase V	Phase W
P1	U1–U2’	V1–V3’	W1–W4’
P2	U1–U2’	V1–V4’	W1–W4’
P3	U1–U3’	V1–V3’	W1–W4’
P4	U1–U3’	V1–V4’	W1–W4’
P5	U1–U4’	V1–V3’	W1–W4’
P6	U1–U4’	V1–V4’	W1–W4’

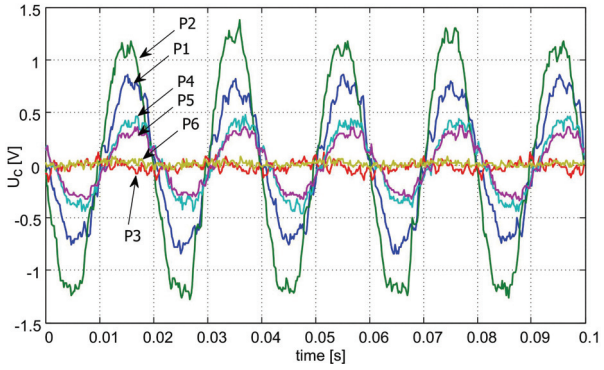

Fig. 3. Waveforms of voltage U_C in cases from P1 to P6

The analysis of selected results of the measured coil voltage

The analysis of waveforms of the measured coil voltage U_C was performed using the following methods: the Discrete Fourier Transform (DFT), the Discrete Stationary Wavelet Transform (DSWT), and the Wavelet Packet Decomposition (WPD).

Discrete Fourier Transform

The Discrete Fourier Transform is realized by Fast Fourier Transform (FFT) in the following form

$$X(k)=\sum_{j=1}^{N} x(j)\omega_N^{(j-1)(k-1)} \tag{1}$$

where $\omega_N = e^{\frac{-2\pi i}{N}}$, N is the length of the signal

The waveforms of voltage U_C were analyzed by FFT. The obtained results of the analysis, i.e. the frequency spectrum of voltage U_C for all cases (from P1 to P6) presented in Table 2 are shown in Fig. 4. It can be seen that the 50Hz frequency can be observed, because of the frequency of the supply voltage.

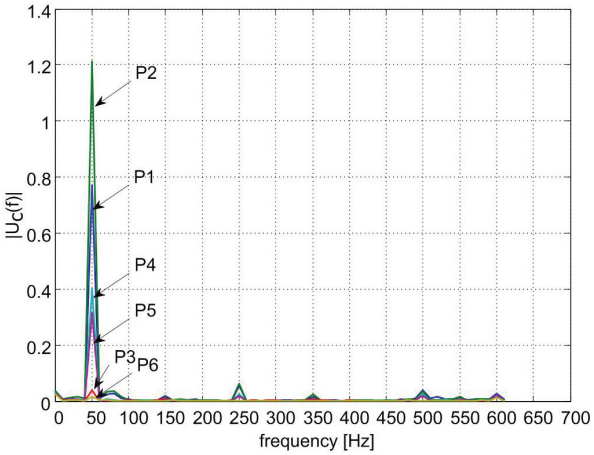

Fig. 4. Spectrum of voltage U_C in cases from P1 to P6

Discrete Stationary Wavelet Transform

The main disadvantage of FFT is the restricted application to stationary signals, i.e. signals without a variation in time. Unfortunately, the faults in the machine could be time-varied, therefore the symptoms are non-stationary signals [7]. In the analysis of non-stationary signals the Wavelet Transform can be used.

The Continuous Wavelet Transform of a signal $x(t)$ is defined as follows

$$\gamma(\tau,s)=\int_{-\infty}^{+\infty} x(t)\frac{1}{\sqrt{s}}\psi^*\left(\frac{t-\tau}{s}\right)dt \tag{2}$$

where: $\psi\left(\frac{t-\tau}{s}\right)$ is a mother wavelet, * is complex conjugation, s is scale, τ is offset.

Using the formula (2) the function $x(t)$ is decomposed into a set of wavelets. The domain of the set is scale-offset. In order to compose the signal $x(t)$, the Inverse Wavelet Transform should be used, which is defined as follows

$$x(t)=\iint \gamma(\tau,s)\cdot\psi\left(\frac{t-\tau}{s}\right)d\tau ds \tag{3}$$

Because the voltage U_C is sampled the Discrete Stationary Wavelet Transform must be used. Generally, this can be done by multiplying voltage U_C and the series of wavelet $\psi_{mn}(t)=s_0^{-\frac{m}{2}}\psi\left(s_0^{-m}t-n\tau_0\right)$. Parameter n locates the analyzed signal in time, while m specifies the top of the frequency range of the signal. In case of parameters $s_0=2$ and $\tau_0=1$ the Dyadic Wavelet Transform is realized. The wavelet analysis can be successfully applied in the diagnosis of rotor asymmetries in induction motors as well as in the analysis of the magnetization vector in permanent magnet machine.

In this work the Discrete Stationary Wavelet analysis was performed using low-pass and high-pass filters in the cases, where the filtration parameters depend on the chosen mother wavelet. In the presented analysis the Daubechies “db3” wavelet was used as mother wavelet. The calculations were performed up to the 3rd level of the decomposition tree (Fig. 5). The result of the analysis was the decomposition of the signal into two components: the approximation and the detail. The obtained approximations of voltage U_C at first (A1), second (A2) and third (A3) level are shown in Fig. 6 and details of voltage U_C at first (D1), second (D2) and third (D3) level are shown in Fig. 7.

The presented analysis of voltage U_C can be found in the process of eliminating interferences in the signal. For further studies, voltage U_C in case P2 of winding asymmetry (Table 2) was chosen.

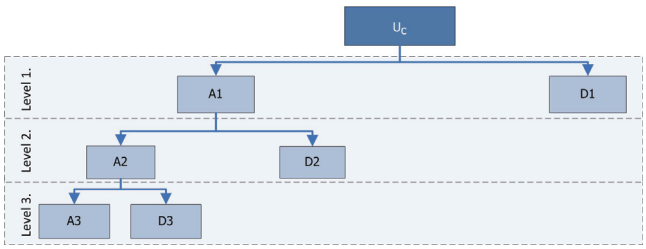

Fig. 5. The decomposition tree with three levels

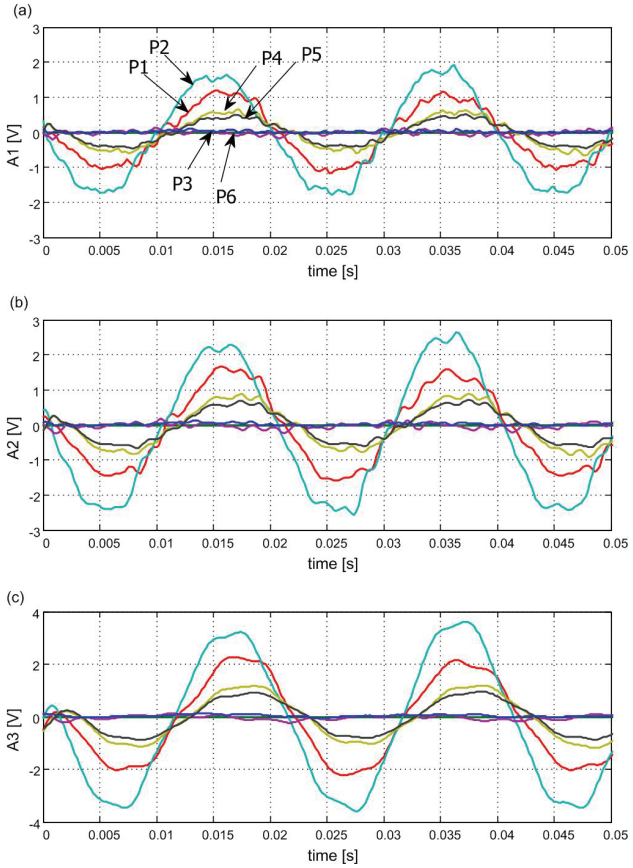

Fig. 6. The approximations of voltage U_C: (a) level 1, (b) level 2 and (c) level 3

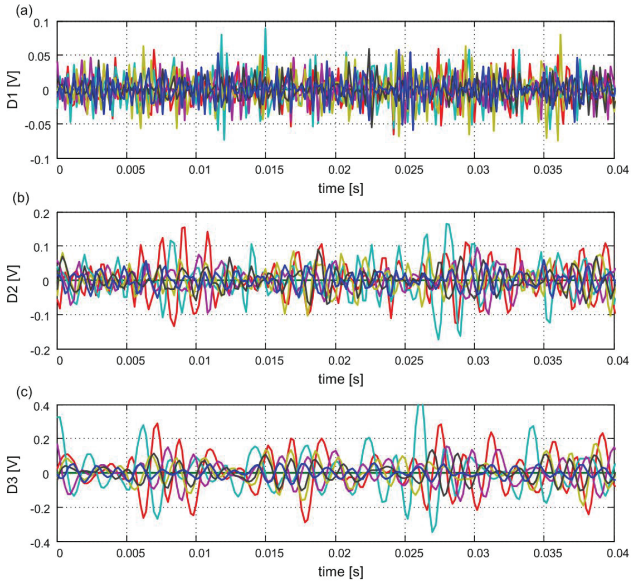

Fig. 7. The details of voltage U_C: (a) level 1, (b) level 2 and (c) level 3

The selected waveform of voltage U_C (case P2 in Table 2) was decomposed to the 5th level of decomposition tree using the Daubechies "db3" wavelet. At each level the approximation and the detail were obtained. On the basis of the components the reconstruction process of the signal waveform was performed. The reconstruction was done by the Inverse Wavelet Transform. The set of waveforms obtained at five levels of reconstruction marked accordingly from L1 to L5 is presented in Fig. 8. However, Fig. 9 shows a part of the waveform for a slice of time from an absolute value of 0.012 s to 0.018 s. On the basis of the above results it can be concluded that the higher level of decomposition, the higher level of distortions removal.

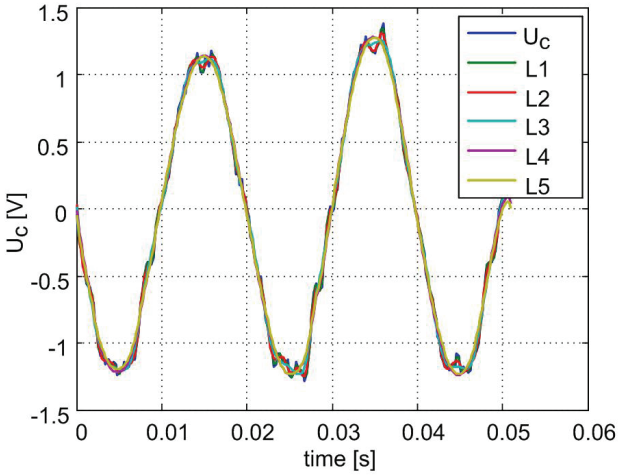

Fig. 8. Reconstruction of the signal at levels L1-L5

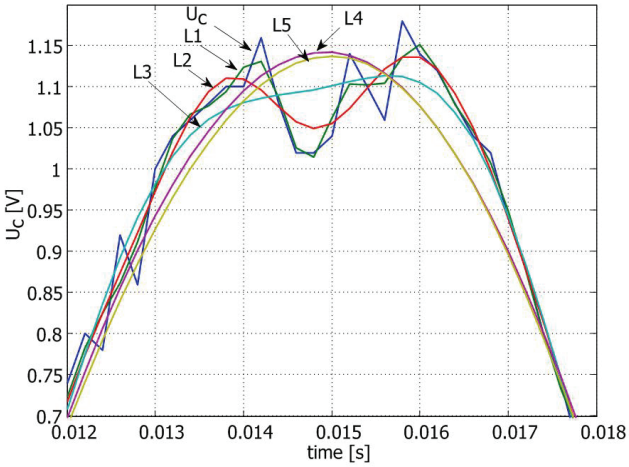

Fig. 9. Reconstruction of the signal at levels L1-L5 from 0.012 s to 0.018 s.

The FFT analysis of reconstructed waveforms (from L1 to L5) was applied to give marks of the reconstruction results and the removing distortions. Fig. 10 shows the results of FFT of the measured voltage U_C and the voltage after the removal of the distortions at levels from L1 to L5. However, Fig. 11 presents the same results for the frequency range from 400 Hz to 800 Hz.

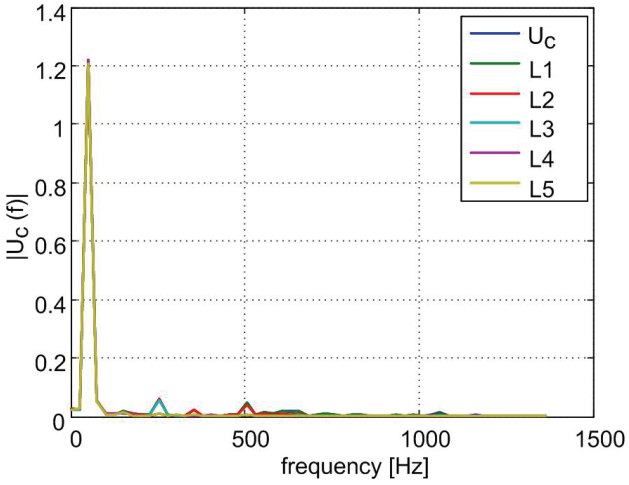

Fig. 10. FFT of the signal after the removal of distortions

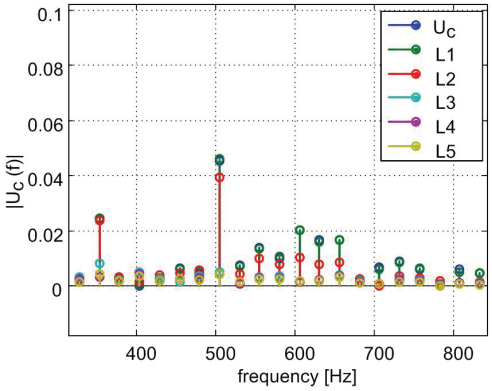

Fig. 11. FFT of the signal after the removal of distortions for the frequency range between 400 Hz and 800 Hz

The amplitudes of the 1st harmonic of the measured voltage U_C and the voltage after the removal of distortions at levels from L1 to L5 were related to the amplitude of the 1st harmonic of voltage U_C. The results are presented in Table 3. On the basis of the obtained results, it can be concluded that the values of the 1st harmonic at levels from L1 to L5 are very close to the value of the 1st harmonic of voltage U_C. Therefore, voltage U_C after the removal of distortions by the Discrete Stationary Wavelet could be used in the diagnostics of electrical machines.

Table. 3. The amplitudes of the signal after the removal of distortions

signal	$\frac{\lvert signal \rvert_{f=50Hz}}{\lvert U_c \rvert_{f=50Hz}}$
UC	100 %
L1	99,9993 %
L2	99,9957 %
L3	99,9910 %
L4	99,9250 %
L5	98,9419 %

Wavelet Packet Decomposition

In the Wavelet Packet Decomposition the signal is split into the approximation and the detail by a low-pass filter and a high-pass filter, respectively. In a successive decomposition level the same steps are repeated for the approximation as well as for the detail (Fig.12).

Applications of the Wavelet Packet Decomposition are widely used in modern analysis of electrical machines, for example in the analysis of the line current of a squirrel cage machine supplied by distorted voltage [8].

In this paper for the Wavelet Packet Decomposition the "db3" wavelet has been applied. The analysis was carried out to the fifth level of the decomposition tree (Fig. 12). At this level we achieved the 2^5=32 nodes of the decomposition tree. Using Shannon formula the value of entropy in each node was calculated. As the results, the set of 32 values was obtained. Therefore, the results are shown in graphical form in Fig. 13. The obtained set of values can be used as the input vector in an artificial neural network for faults detection in electrical machines [4].

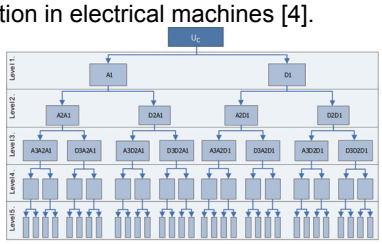

Fig. 12. Tree of wavelet packet decomposition

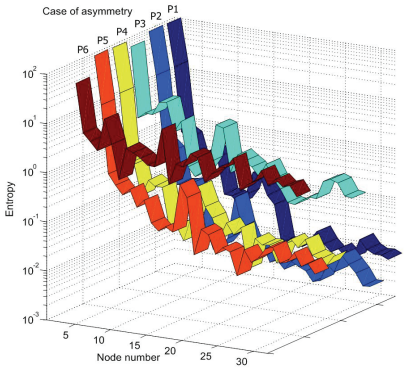

Fig. 13. The entropy of nodes in decomposition tree at the 5th level

Summary

The paper presents the analysis of a waveform of voltage induced in a search coil placed perpendicularly to the shaft in the vicinity of stator winding end-turns. As can be seen, a coil was used to measure the axial flux. In order to obtain the axial flux, the asymmetry in stator winding was modeled. The measured waveforms of voltage U_C were analyzed using the following methods: the Fast Fourier Transform (FFT), the Discrete Stationary Wavelet Transform (DSWT), and the Wavelet Packet Decomposition (WPD). On the basis of the results it can be concluded that the DSWT could effectively remove distortions of the measured voltage. The results obtained by the WPD can be used as the input vector in an artificial neural network. The DSWT and the WPD could be successfully used in the preconditioning process in diagnostics of electrical machines.

REFERENCES

[1] Douglas H., Pillay P., Barendse P., The Detection of Interturn Stator Faults in Doubly-Fed Induction Generators, Industry Applications Conference,. Fourtieth IAS Annual Meeting. Conference Record of the 2005, Vol. 2, 2005, pp. 1097–1102.

[2] Kia S. H., Henao H., Capolino G. A., Diagnosis of Broken-Bar Fault in Induction Machines Using Discrete Wavelet Transform Without Slip Estimation, IEEE Transactions On Industry Applications, Vol. 45, No. 4, 2009, pp. 1395-1404.

[3] Pietrowski W., Application of radial basis neural network to diagnostics of induction motor stator faults using axial flux, Electrical Review, Vol. 87, No. 6, 2011, pp.190-192.

[4] Bellini A., Filippetti F., Tassoni C., Capolino G. A., Advances in Diagnostic Techniques for Induction Machines, IEEE Transactions On Industrial Electronics, Vol. 55, No. 12, 2008, pp.4109-4126.

[5] Bonnett A. H., Soukup G. C., Cause and Analysis of Stator and Rotor Failures in Three-phase Squirrel-Cage Induction Motors, IEEE Transactions On Industry Applications, Vol. 28, No. 4, 1992, pp. 921-937.

[6] Bacha K., Henaob H., Gossa M., Capolino G. A., Induction machine fault detection using stray flux EMF measurement and neural network-based decision, Electric Power Systems Research 78, 2008, pp. 1247–1255.

[7] Riera-Guasp M., Antonino-Daviu J., Rusek J., Roger-Folcha J., Diagnosis of rotor asymmetries in induction motors based on the transient extraction of fault components using filtering techniques, Electric Power Systems Research 79, Elsevier, 2009, pp. 1181–1191.

[8] Barański M., Pietrowski W., The wavelet packets analysis of phase current of squirrel cage motor supplied with distorted voltage, Proc. XIX Symposium Electromagnetic Phenomena in Nonlinear Circuits, 28-30 June 2006, Maribor, Slovenia, pp.23-24.

***Author**: dr inż. Wojciech Pietrowski, Poznan University of Technology, Institute of Electrical Engineering and Electronics, ul. Piotrowo 3A, 60-965 Poznan, Poland, E-mail: wojciech.pietrowski@put.poznan.pl;*